JOURNAL OF NANO- AND ELECTRONIC PHYSICS
Vol. 7 No 2, 02021(5pp) (2015)

ЖУРНАЛ НАНО- ТА ЕЛЕКТРОННОЇ ФІЗИКИ
Том 7 № 2, 02021(5cc) (2015)

High-frequency Conductivity of Carbon Nanotubes of Zigzag-configuration

A.V. Korotun[1,*], I.M. Titov[2], Ya.V. Karandas[1]

[1] Zaporizhzhya National Technical University, 64, Gogol Str., 69063 Zaporizhzhya, Ukraine
[2] Taurian State Agrotechnology University, 18, B. Khmelnitsky Pr., 72310 Melitopol, Ukraine

(Received 25 March 2015; published online 10 June 2015)

The frequency dependences of the surface conductivity of carbon nanotubes of zigzag-configuration have been investigated in the single-electron approximation. The calculations have been performed for nanotubes with semiconductor and metallic conductivity. The influence of chirality on the total conductivity and its individual components has been analyzed.

Keywords: Carbon nanotubes, Chirality, Conductivity, Interband transitions, Frequency, Oscillations.

PACS numbers: 73.22. – f, 73.25. + i, 73.63.Fg

1. INTRODUCTION

Development of modern nanoelectronics creates the basis for a new step in solving the problem of miniaturization of the data transmission, receiving and processing devices. The use of the latest advances in molecular electronics which manipulates single atoms and molecules is one of these steps. It is based on the use of new nanomaterials, such as fullerenes and carbon nanotubes [1-7], organic polymers [8], structures on the basis of quantum wells, wires and quantum dots [9]. Such systems are the nanoscale inhomogeneities of different nature and configuration, which provide a spatial restriction of charge carrier motion in one or several directions.

Spatial quantization of the electron motion leads to discretization of the energy spectrum with energy levels determined by size and shape of the nanostructure. This effect, in particular, conditions a unique property of single-walled carbon nanotubes of zigzag-configuration to change own conductivity by several orders of magnitude, from semiconductor to metallic one, by changing the radius by a few angstroms [10].

Except the effect of spatial restriction of charge carrier motion, typical for nanostructures spatial inhomogeneity creates in them nanoscale inhomogeneities of electromagnetic fields. In many cases they generate a significant spatial dispersion that plays a substantial role in materials optics [11]. High-frequency conductivity is one of the main optical characteristics of carbon nanotubes.

Thus, the aim of this work is to study the behavior of high-frequency conductivity of carbon nanotubes of zigzag-configuration with different chirality.

2. STATEMENT OF THE PROBLEM

Let us consider a single-layer carbon nanotube whose axis is oriented along the z-axis of the Cartesian coordinate system. We assume that a plane electromagnetic wave $\mathbf{\mathcal{E}}(t) = \mathbf{e}_z\mathcal{E}_0 e^{-i\omega t}$ polarized along the nanotube axis is incident on the nanotube, and the wave number $\mathbf{k}$ (and, correspondingly, direction of the wave propagation) is perpendicular to the carbon nanotube axis. Electromagnetic wave excites in the carbon nanotube electric current of the density of $\mathbf{j}(t) = \mathbf{e}_z j_0(\omega) e^{-i\omega t}$. Hereinafter, we will assume that wavelength $\lambda = 2\pi/|\mathbf{k}|$ is much larger than the radius of the carbon nanotube, but is much less than its length L. In this case, amplitude of the current (induced in the nanotube) density $j_0(\omega)$ and amplitude of the plane wave $\mathcal{E}_0$ are connected by the relation

$$j_0(\omega) = \sigma(\omega)\mathcal{E}_0, \qquad (1)$$

where $\sigma(\omega)$ is the surface conductivity of the carbon nanotube, which in the single-electron approximation can be written in the form of [12]

$$\sigma(\omega) = \sigma_1(\omega) + \sigma_2(\omega), \qquad (2)$$

where

$$\sigma_1(\omega) = \frac{e^2}{2\pi^2\hbar\left(\mathrm{i}\,\omega - \frac{1}{\tau}\right)R}\sum_{s=1}^{m}\int_{-a}^{a}\frac{\partial\varepsilon_c(p,s)}{\partial p}\frac{\partial}{\partial p}\left\{f\left[\varepsilon_c(p,s)\right] - f\left[-\varepsilon_c(p,s)\right]\right\}dp\,, \qquad (3)$$

$$\sigma_2(\omega) = \frac{\mathrm{i}\,\omega e^2}{\pi^2\hbar^2 R}\sum_{s=1}^{m}\int_{-a}^{a}\frac{\omega_{cv}(p,s)\mathcal{R}_{cv}^2(p,s)\left\{f\left[\varepsilon_c(p,s)\right] - f\left[-\varepsilon_c(p,s)\right]\right\}}{\omega_{cv}^2(p,s) - \left(\omega + \frac{\mathrm{i}}{\tau}\right)}dp \qquad (4)$$

are the parts of the surface conductivity conditioned by the intraband and interband transitions, respectively. In (3), (4): τ is the relaxation time, $R = \left(\sqrt{3}b\sqrt{m^2 + mn + n^2}\right)/2\pi$ is the radius of the single-layer nanotube; m, n are the chirality indices; $b = 0.142$ nm is the interatomic distance in the crystal lattice of graphene; p is the quasi-momentum of electrons varied in the range of $-a \le p \le a$;

$$f\left[\varepsilon_c(p,s)\right] = \left\{\exp\left(\frac{\varepsilon_c(p,s)}{k_B T}\right) + 1\right\}^{-1} \qquad (5)$$

---

[*] andko@zntu.edu.ua

is the Fermi-Dirac distribution; T is the temperature of the electron subsystem of the carbon nanotube;

$$\varepsilon_c\left(p,s\right)=\gamma_0\sqrt{1+4\cos\frac{3pb}{2\hbar}\cos\frac{\pi s}{m}+4\cos^2\frac{\pi s}{m}} \qquad (6)$$

is the dispersion low of motion of π-electrons in the conduction band, $\gamma_0 = 2.7$ eV is the overlap integral;

$$\omega_{cv}\left(p,s\right)=\frac{2\varepsilon_c\left(p,s\right)}{\hbar} \qquad (7)$$

is the frequency of the interband transitions;

$$\mathcal{R}_{cv}\left(p,s\right)=-\frac{b\gamma_0^2}{2\varepsilon_c^2\left(p,s\right)}\left(1+\cos\frac{3pb}{2\hbar}\cos\frac{\pi s}{m}-2\cos^2\frac{\pi s}{m}\right) \qquad (8)$$

is the matrix element of the dipole moment operator of the carbon nanotube [13].

Calculating the derivatives with respect to momentum and substituting the obtained results into (3), after some mathematical transformations we have

$$\sigma_1\left(\omega\right)=-\frac{e^2}{2\pi^2\hbar R\left(\omega^2+\dfrac{1}{\tau^2}\right)}\left(\frac{1}{\tau}+\mathrm{i}\,\omega\right)\mathcal{I}_1, \qquad (9)$$

where the following designation is introduced:

$$\mathcal{I}_1=-\frac{9\gamma_0^3 b^2}{\hbar^2 k_B T}\sum_{s=1}^{m}\cos^2\frac{\pi s}{m}\int_{-a}^{a}\frac{\sin^2\dfrac{3pb}{2\hbar}}{\varepsilon_c\left(p,s\right)\mathrm{ch}^2\left(\dfrac{\varepsilon_c\left(p,s\right)}{2k_B T}\right)}dp. \qquad (10)$$

Substituting formulas (5)-(8) into (4) and separating the real and imaginary parts, we obtain

$$\sigma_2\left(\omega\right)=\frac{e^2\gamma_0^4\omega}{\pi^2\hbar^3 R}\sum_{s=1}^{m}\left(\frac{\omega}{\tau}\mathcal{I}_2+\frac{\mathrm{i}}{2}\mathcal{I}_3\right), \qquad (11)$$

where

$$\mathcal{I}_2=\sum_{s=1}^{m}\int_{-a}^{a}\frac{\left(1+\cos\dfrac{3bp}{2\hbar}\cos\dfrac{\pi s}{m}-2\cos^2\dfrac{\pi s}{m}\right)}{\left[\left(\dfrac{4\varepsilon_c^2\left(p,s\right)}{\hbar^2}-\omega^2+\dfrac{1}{\tau^2}\right)^2+\dfrac{4\omega^2}{\tau^2}\right]\varepsilon_c^3\left(p,s\right)}\mathrm{th}\left(\frac{\varepsilon_c\left(p,s\right)}{2k_{\mathrm{B}}T}\right)dp; \qquad (12)$$

$$\mathcal{I}_3=\sum_{s=1}^{m}\int_{-a}^{a}\frac{\left[\dfrac{4\varepsilon_c^2\left(p,s\right)}{\hbar^2}-\omega^2+\dfrac{1}{\tau^2}\right]\left(1+\cos\dfrac{3bp}{2\hbar}\cos\dfrac{\pi s}{m}-2\cos^2\dfrac{\pi s}{m}\right)}{\left[\left(\dfrac{4\varepsilon_c^2\left(p,s\right)}{\hbar^2}-\omega^2+\dfrac{1}{\tau^2}\right)^2+\dfrac{4\omega^2}{\tau^2}\right]\varepsilon_c^3\left(p,s\right)}\mathrm{th}\left(\frac{\varepsilon_c\left(p,s\right)}{2k_{\mathrm{B}}T}\right)dp. \qquad (13)$$

In the sequel, we will use formulas (9) and (11) for the calculations of the high-frequency surface conductivity of nanotubes of different chirality.

3. CALCULATION RESULTS AND DISCUSSION

Calculation was performed for the nanotubes of zigzag-configuration at room temperature in the case, when relaxation time is equal to $\tau = 3{\cdot}10^{-14}$ s.

In Fig. 1 we present the dependences of the real and imaginary parts of the intraband conductivity on the frequency for carbon nanotubes with chiralities (14.0) and (15.0). As seen from the figure, behavior of the real part of the conductivity for these nanotubes coincides qualitatively. However, they differ quantitatively by about two orders of magnitude because of higher occupancy of the conduction band in the case of a nanotube with metallic conductivity. A similar picture also takes place for the imaginary part of the intraband conductivity. Difference in the behavior between $\mathrm{Im}\sigma_1$ and $\mathrm{Re}\sigma_1$ consists only in the fact that $\mathrm{Im}\sigma_1$ at relatively small frequencies increases to the maximum, which takes place at $\omega \approx 5{\cdot}10^{13}$ s^{-1}, while $\mathrm{Re}\sigma_1$ permanently decays. This fact is conditioned by the increase in the intensity of the transitions at the given frequency.

For the interband conductivity (Fig. 2) oscillations of both the real and imaginary parts take place. At that, for the case of metallic nanotubes oscillations of the real part start at $\omega \approx 5{\cdot}10^{14}$ s^{-1}, and for semiconductor ones – at $\omega \sim 10^{15}$ s^{-1}. Oscillations appear in the case, when electromagnetic wave frequency coincides with the frequency of the electron interband transitions. Oscillation amplitude of $\mathrm{Re}\sigma_2$ is large for nanootubes with chirality (14.0). Oscillations of $\mathrm{Im}\sigma_2$ of nanotubes with (15.0) start at $\omega \approx 2.7{\cdot}10^{15}$ s^{-1}, and of nanotubes with (14.0) – at $\omega \sim 10^{15}$ s^{-1} that is explained by a larger value of $\varepsilon_c(p, s)$ for nanotubes with metallic conductivity at fixed p and s.

In Fig. 3 we show the frequency dependences of the "total" conductivity for nanotubes with chirality (14.0) and (15.0). Oscillation amplitudes of the imaginary part are one order of magnitude less than the oscillation amplitudes of the real part. Moreover, oscillations of $\mathrm{Re}\sigma$ for a nanotube with metallic conductivity start at smaller frequencies than for a nanotube with semiconductor conductivity and have a larger period and less amplitude (see Fig. 3a). While for the $\mathrm{Im}\sigma$ – vice versa – in the case of metallic nanotubes oscillations are exhibited at higher frequencies than for semiconductor ones, and their amplitudes and periods are almost equal (Fig. 3b).

In contrast to the high-frequency range, in the low-frequency range ($\omega < 10^{15}$ s^{-1}) conductivities of semiconductor and metallic carbon nanotubes differ significantly from each other. Thus, the real part of the conductivity of nanotubes with (15.0) decreases with decreasing field frequency reaching the minimum at $\omega \approx 6{\cdot}10^{14}$ s^{-1}, and then it increases by two orders of magnitude. For nanotubes with (14.0), $\mathrm{Re}\sigma$ also decreases with decreasing frequency reaching the minimum at $\omega \approx 10^{14}$ s^{-1}, and then it slightly increases. This is conditioned by the fact that contribution of the interband motion of electrons to the conductivity decreases with decreasing frequency. In this case, contribution of the intraband motion of elect-

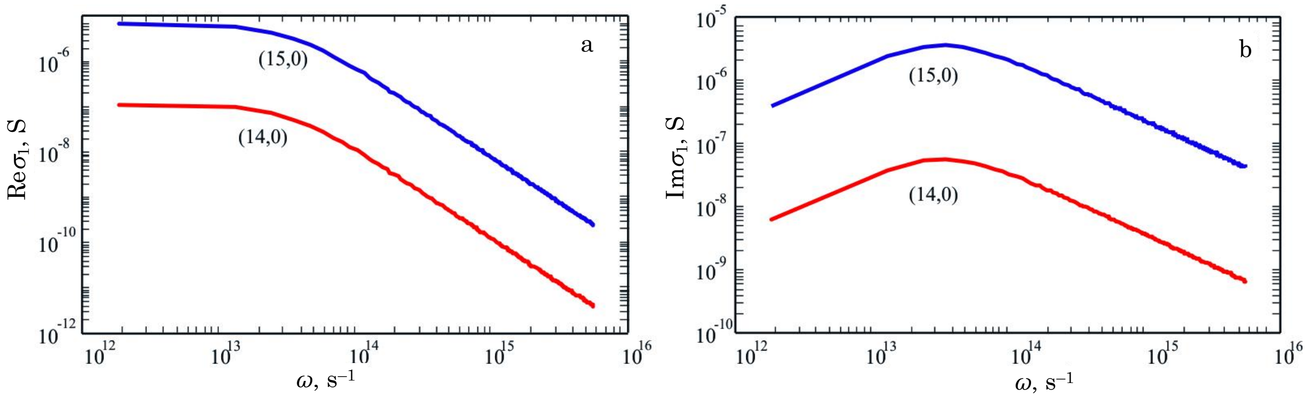

Fig. 1 – Frequency dependences of the real (a) and imaginary (b) parts of the intraband conductivity of carbon nanotubes with chiralities (14.0) and (15.0)

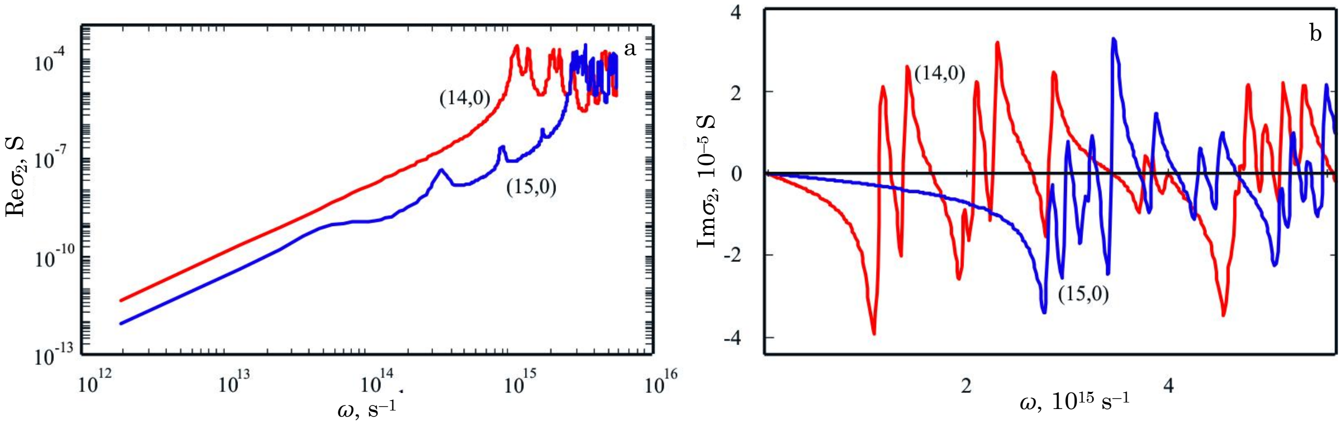

Fig. 2 – Frequency dependences of the real (a) and imaginary (b) parts of the interband conductivity of carbon nanotubes with chiralities (14.0) and (15.0)

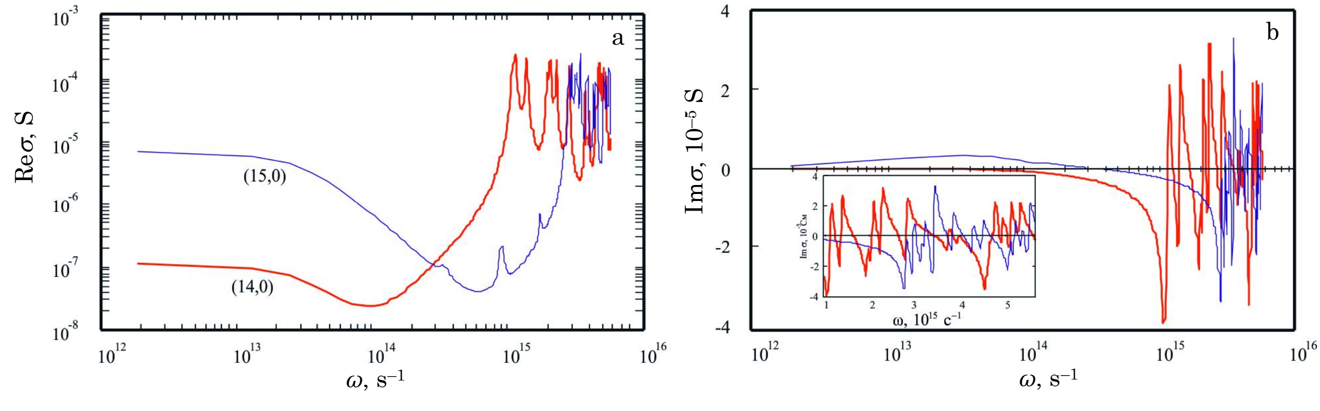

Fig. 3 – Frequency dependences of the real (a) and imaginary (b) parts of the "total" conductivity of carbon nanotubes with chiralities (14.0) and (15.0)

rons becomes the dominant one. In connection with the fact that density of electronic states in the vicinity of the Fermi level of metallic carbon nanotubes is not equal to zero, contribution of the intraband motion of electrons to the conductivity of metallic nanotubes is large that leads to larger values of the conductivity. In semiconductor nanotubes, density of states in the vicinity of the Fermi level is equal to zero that leads to a weak occupancy of the conduction band of the given types of nanotubes at room temperature and, correspondingly, to a very small contribution of the intraband motion of electrons to the conductivity. Because of the fact that in the low-frequency range contribution of the intraband motion of electrons to the conductivity of metallic nanotubes dominates over the contribution of the interband transitions, then for the calculation of the metallic nanotube conductivity in this range we can neglect the second term in expression (2).

In Fig. 4 we illustrate the dependences Re$\sigma_1(\omega)$ and Im$\sigma_1(\omega)$ of carbon nanotubes with (2.0) and (3.0). Behavior of the real part of the conductivity for nanotubes with semiconductor and metallic properties coincides qualitatively. However, they differ in magnitude by about 20 orders that is explained by a weak occupancy of the conduction band of these nanotubes. If compare Fig. 4 and Fig. 1 we see that the real part of the conductivity of metallic nanotubes has the following behavior with

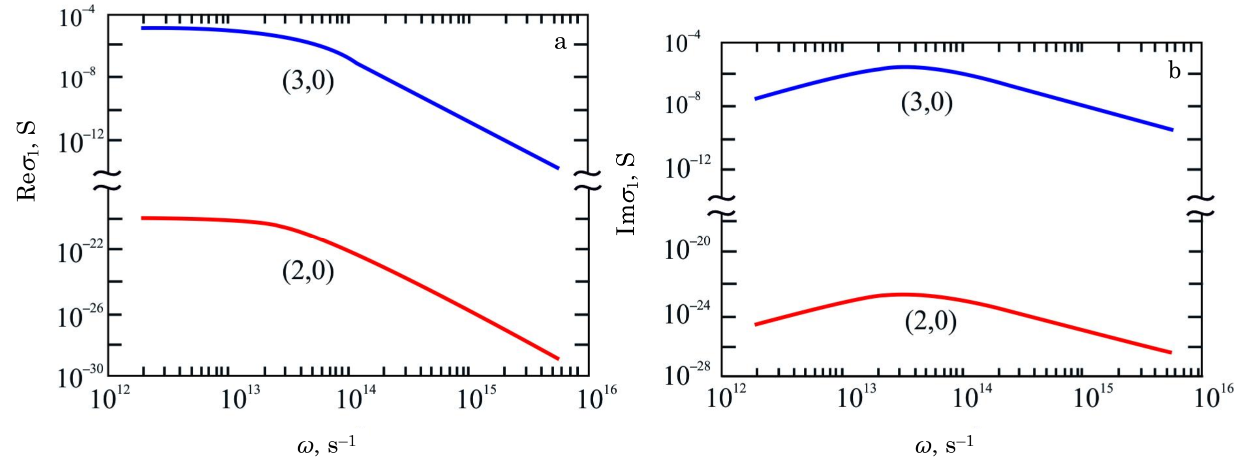

Fig. 4 – Frequency dependences of the real (a) and imaginary (b) parts of the intraband conductivity of carbon nanotubes with chiralities (2.0) and (3.0)

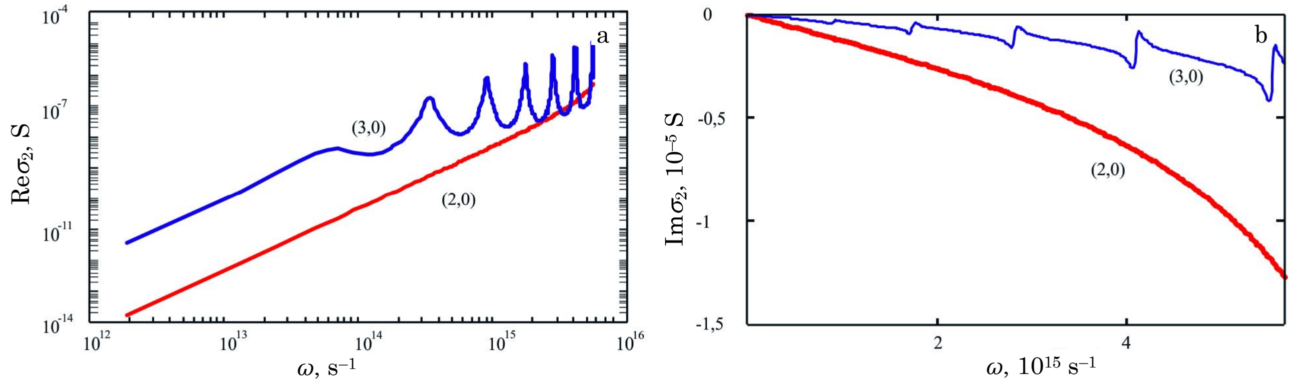

Fig. 5 – Frequency dependences of the real (a) and imaginary (b) parts of the interband conductivity of carbon nanotubes with chiralities (2.0) and (3.0)

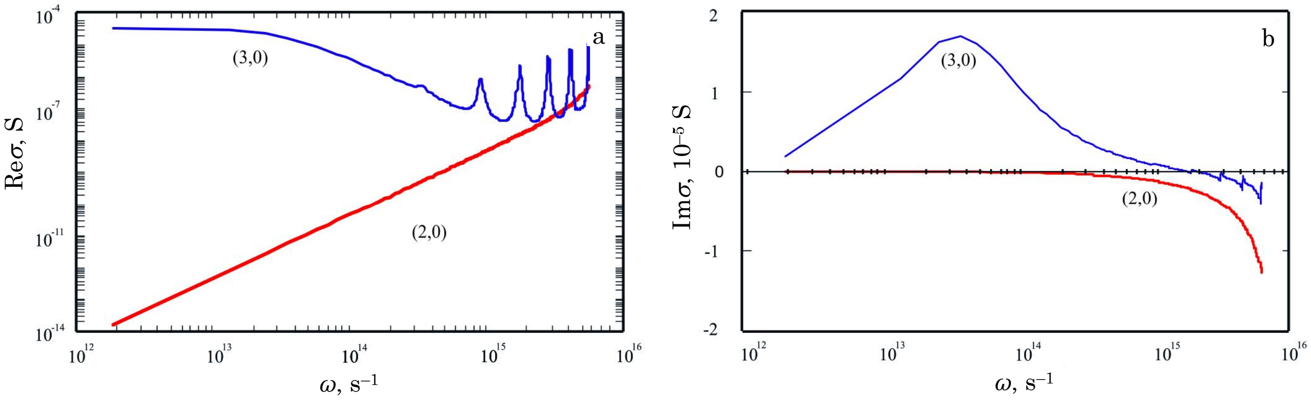

Fig. 6 – Frequency dependences of the real (a) and imaginary (b) parts of the "total" conductivity of carbon nanotubes with chiralities (2.0) and (3.0)

decreasing chirality indices: at $\omega \sim 10^{12} \div 10^{13}$ s^{-1} they almost do not differ, and at higher frequencies decrease in the conductivity for nanotubes with larger chirality index is more significant. Behavior of $\mathrm{Re}\sigma_1$ for the case of nanotubes with semiconductor conductivity and chiralities (2.0) and (14.0) is qualitatively similar, but they differ in magnitude by 18 orders. For the imaginary part of the intraband conductivity dependences are also similar. However, in the case of smaller chiralities, the maximum is less pronounced. The picture is quantitatively the same as for the real part: for metallic nanotubes the value of $\mathrm{Im}\sigma_1$ is close and for semiconductor nanotubes it differs by 18 orders. Such a substantial difference in the values of the conductivity for semiconductor nanotubes is conditioned by the band structure features.

Fig. 5 shows the behavior of the real and imaginary parts of the interband conductivity for nanotubes with chiralities (2.0) and (3.0). The real part of the conductivity of nanotubes with semiconductor properties monotonously increases and the imaginary one monotonously decreases with increasing frequency. Oscillations of both the real (starting from $\omega \sim 10^{14}$ s^{-1}) and imaginary parts take place for metallic nanotubes in contrast to the semiconductor ones. At that, with increasing frequency the oscillation amplitude of Reσ_2 increases and their period decreases, while for Imσ_2 both the oscillation period and their amplitude increase. Explanation of this fact is similar to the case of the interband conductivity of nanotubes with chiralities (14.0) and (15.0).

For the total conductivity of nanotubes with chirality (3.0) (Fig. 6a) one can observe the decay of the real part to $\omega \sim 10^{15}$ s^{-1}, and then the increase with oscillations (period decreases and amplitude increases with increasing ω). In the case of semiconductor nanotubes, Reσ monotonously increases all the time that is explained by the dominant role of the interband conductivity. The imaginary part of the total conductivity of nanotubes with chirality (2.0) remains almost constant till the frequency of $\omega \sim 10^{15}$ s^{-1}, and then it sharply decreases. For nanotubes with chirality (3.0), the imaginary part has the following behavior: at first, it increases to the maximum at $\omega \simeq 3{\cdot}10^{13}$ s^{-1}, then it decays, and weak oscillations are observed at $\omega \simeq 2{\cdot}10^{15}$ s^{-1}. Thus, at frequencies of $\omega < 2{\cdot}10^{15}$ s^{-1}, the main contribution to the total conductivity of nanotubes with chiralities (2.0) and (3.0) is determined by the intraband conductivity, and at higher frequencies – by the interband one.

4. CONCLUSIONS

It is shown that behavior of the real and imaginary parts of the intraband conductivity of nanotubes with different types of conductivity qualitatively coincides. However, they substantially differ quantitatively due to higher occupancy of the conduction band.

Oscillations of both the real and imaginary parts, the reason of which is the proximity of the electromagnetic wave frequency to the frequency of the interband electron transitions, take place for the interband conductivity of nanotubes with large chiralities. At that, for the case of metallic nanotubes, oscillations of the real part start at lower frequencies. For nanotubes with small chiralities, oscillations of the conductivity occur only for the metallic nanotubes.

It is established that behavior of the real and imaginary parts of the total conductivity in the low-frequency range for the case of metallic and semiconductor nanotubes is significantly different. This is conditioned by the fact that with decreasing frequency, contribution of the interband transitions to the conductivity decreases, and contribution of the intraband transitions becomes the dominant one. Oscillations of the real and imaginary parts of the total conductivity in high-frequency range for semiconductor nanotubes, in contrast to the metallic ones, take place only for the case of large chiralities.

REFERENCES

1. M.S. Dresselhaus, G. Dresselhaus, P.C. Eklund, *Science of fullerenes and carbon nanotubes* (New York: Academic press: 1996).
2. M.S. Dresselhaus, G. Dresselhaus, Ph. Avouris, *Carbon nanotubes* (Berlin Heidelberg: Springer-Verlag: 2001).
3. M.V. Shuba, G.Ya. Slepyan, S.A. Maksimenko, C. Thomson, A. Lakhtakia, *Phys. Rev. B* **79**, 155403 (2009).
4. M.B. Belonenko, S.Yu. Glazov, N.E. Mescheryakova, *Semiconductors* **44**, 1211 (2010).
5. K.G. Batrakov, O.V. Kibis, P.P. Kuzhir, M.R. da Costa, M.E. Portnoi, *J. Nanophoton.* **4**, 041665 (2010).
6. Qi. Zhang, E.H. Hároz, Z. Jin, L. Ren. X. Wang, R.S. Arvidson, A. Lüttge, Ju. Kono, *Nano Lett.* **13**, 5991 (2013).
7. N.R. Sadykov, *Tech. Phys.* **59**, 1191 (2014).
8. *Printed organic and molecular electronics* (Eds. D.R. Gamota, P. Brazis. K. Kalyanasundaram, J. Zhang) (Massachusetts: Kluwer Academic Press: 2004).
9. M.J. Kelly, *Low-dimensional semiconductors: materials, physics, technology, devices* (New York: Clarendon Press: 1995).
10. P.N. D'yachkov, *Elektronnyye svoystva i primeneniye nanotrubok* (Moskva: Binom: 2011).
11. V.M. Agranovich, V.L. Ginzburg, *Kristallooptika s uchetom prostranstvennoy dispersii i teoriya eksitonov* (Moskva: Nauka: 1979).
12. *Electrodynamic properties of carbon nanotubes. Electromagnetic Fields in Unconventional Structures and Materials* Ed. O.N. Singh, A. Lakhtakia (New York: John Wiley & Sons, Inc: 2000).
13. A.M. Nemilentsev, G.Ya. Slepyan, S.A. Maksimenko, *Vestnik BGU. Ser. 1*, No3, 18 (2008).